Journal of the European Ceramic Society 16 (1996) 211–215

0955-2219(95)00154-9
0955-2219/96/$15.00

Electron Paramagnetic Resonance and Optical Absorption Studies on Cr-doped Mullite Precursors

H. Schneider,[a] K. Ikeda,[b] B. Saruhan[a] & H. Rager[c]

[a]Institute for Materials Research, German Aerospace Research Establishment, 51140 Köln, Germany
[b]Department of Advanced Material Science and Engineering, Yamaguchi University, 755 Ube, Japan
[c]Department of Geosciences, University of Marburg, 35032 Marburg, Germany

(Accepted 22 July 1995)

Abstract

Mullite precursors doped with 3 wt% Cr_2O_3 were investigated with X-ray diffractometry (XRD), electron paramagnetic resonance (EPR) and optical absorption spectroscopy. The development of phase assemblages occurs over three temperature ranges. In the first temperature field (450–600°C) the precursors are amorphous, and in the second field (800–1100°C) small amounts of γ-Al_2O_3 and crystalline Cr_2O_3 can be observed. Finally, in the third field (≥1250°C) mullite forms, and simultaneously γ-Al_2O_3 and crystalline Cr_2O_3 disappear.

The EPR measurements reveal different temperature-controlled structural types of short-range order of Cr in the precursors, which go along with phase developments. Between 450 and 800°C EPR spectra appear with a main signal at $g_{eff} \approx 1{\cdot}96$, most probably resulting from Cr^{5+}. Between 800 and 1250°C, the Cr EPR signal is similar to that of Cr-containing glasses, and above 1250°C the typical Cr^{3+} EPR spectrum of Cr-doped mullite appears.

Optical absorption spectroscopy yields evidence for the occurrence of Cr^{6+}, Cr^{5+} and Cr^{3+} in the mullite precursors, the concentrations of the different oxidation states being dependent on the calcination temperature: Cr^{6+} and Cr^{5+} contents are high at low temperatures (450°C), but gradually decrease with temperature. Simultaneously, increasing amounts of Cr^{3+} can be detected. At temperatures >1100°C, Cr^{6+} and Cr^{5+} cations completely disappear and optical absorption and EPR spectra of samples gradually approach to those of Cr-doped mullite. Although starting materials consist of Cr^{3+}, slow hydrolysis kinetics of Cr^{3+} causes formation of polyanions which contain Cr^{6+}. Deprotonation on heating results in reduction of $[Cr_2^{6+}O_7]^{2-}$ species to form $Cr_2^{3+}O_3$.

Introduction

Syntheses of high purity and ultra-reactive sol–gel mullite precursor powders have become important for the fabrication of advanced mullite ceramics.[1,2] These materials exhibit outstanding mechanical, optical and electrical properties suitable for high temperature optical windows, for substrates in multilayer computer packaging, for high temperature insulating devices, and for high temperature structural applications in aircraft turbine engines and space vehicles.[3,1]

Previous studies have shown that three different types of mullite formation processes can be distinguished in precursors of stoichiometric 3:2 mullite composition (72 wt% Al_2O_3, 28 wt% SiO_2), designated as mullite precursor types I, II and III.[4] Type I and type III precursors are amorphous at room temperature and remain so up to 900°C. Above this temperature, type I precursors crystallize to Al_2O_3-rich mullite, while precursors of type III transform to γ-alumina and, consequently, mullite formation follows at temperatures ≥1200°C. Type II precursors consist of poorly crystalline pseudo-boehmite at room temperature which transforms to γ-alumina above ~350°C. Mullite crystallization occurs at temperatures ≥1200°C.[4,5] The different crystallization behaviours of mullite precursors were attributed to different structural short-range orders prior to mullite formation.

The aim of this study was to provide knowledge on the temperature-dependent development of the structural order of mullite precursors which are doped with paramagnetic and optically absorbant Cr ions. A specific goal was to investigate local structures of the precursors using Cr ions occurring in different oxidation states as probes. For that purpose X-ray diffractometry (XRD),

electron paramagnetic resonance (EPR) and optical absorption spectroscopy were applied.

Experimental Methods

Sample preparation

Cr-doped precursors were synthesized from purely organic starting materials. Tetraethoxysilane (TEOS) and aluminium-sec-butylate ($Al-(OBu^S)_3$) were separately diluted with isopropanol and then admixed in proportions corresponding to 3:2 mullite (72 wt% Al_2O_3, 28 wt% SiO_2). Chromium(III) acetate was dissolved in ethanol at ~80°C. The solution was homogenized for 1 h using a magnetic stirrer and was added to the alcoholic mixed solution of TEOS and $Al-(OBu^S)_3$. The addition of Cr corresponds to 3 wt% Cr_2O_3 in the final product. After further homogenization, hydrolysis was carried out by addition of deionized acidic water. Its pH was adjusted to 1·5 with HCl. Gelation took place immediately after hydrolysis. The gel was dried over several hours in a sandbath at 110°C and a very fine and greenish precursor powder was obtained. The precursor was calcined in a temperature range between 450 and 1750°C (Table 1).

X-ray diffractometry (XRD)

X-ray powder diffractometry studies were carried out with a computer-controlled Siemens D5000 powder diffractometer using Ni-filtered Cu K_α radiation. Diffraction patterns were recorded in the 10 to 80° 2θ range, in the step scan mode (3 s/0·02°, 2θ).

Table 1. Heat treatments of Cr-doped mullite precursors

Sample key	*Temperature (°C)*	*Duration (h)*	*Colour of powder*
CR3-450	450	15	Yellow
CR3-600	600	15	Greenish yellow
CR3-800	800	15	Pale green
CR3-900	900	15	Greyish pale green
CR3-950	950	15	Greyish pale green
CR3-1100	1100	15	Greyish pale green
CR3-1650	1650	15	Grey
CR3-1750	1750	2	Grey

Electron paramagnetic resonance spectroscopy (EPR)

EPR measurements were performed on powder samples at room temperature. The spectra were recorded at both X-band (9·5 GHz) and Q-band (35 GHz) frequency, using a magnetic modulation of 100 kHz and 5×10^{-4} T. Some selected samples were also measured at low temperatures down to 50 K in order to check unknown paramagnetic species in the precursor samples.

Optical absorption spectroscopy

Unpolarized diffuse reflectance spectra were recorded for the precursor series in the wavelength range 290 nm (34 400 cm^{-1}) to 1538 nm (6500 cm^{-1}). A Hitachi 323S automatic recording spectrophotometer with an integrating globe was used. $BaSO_4$ was taken as reference material. Reading the original analogous spectra by a digitizer in 100 cm^{-1} intervals, digital spectra were obtained, and stored in a computer. The Kubelka–Munk function was applied. Before evaluation of the spectra a baseline correction in both the infra-red (IR) and ultraviolet (UV) region was carried out using Gaussian curves with centres around 3400 and 34 000 cm^{-1}. Around these wavenumbers, vibronic bands of H_2O and M–O charge transfer bands occur. Overtone bands of adsorbed H_2O appearing around 6900 cm^{-1} were corrected by a smoothing procedure. On the basis of known crystal field absorption bands of Cr^{3+} in Cr_2O_3–SiO_2 gels and glasses,[6] the obtained spectra were fitted with a Gaussian peak fitting procedure. Bands due to Fe^{2+} around 10 000 cm^{-1} were included into the fitting procedure. High energy absorption bands of Cr^{3+} originating from the crystal field P term were also taken into account. These extra bands are labelled R, F, U, 9 and 10 (Table 2). All spectra fittings were carried out assuming a cubic crystal field.

Table 2. Optical absorption band peak positions of Cr-doped mullite precursors heat-treated at different temperatures

Sample key	*Absorption band (cm^{-1})*													
	R	*F*	*1*	*2*	*3*	*4*	*5*	*6*	*7*	*8*	*9*	*10*	*U*	σ
CR3-450	3400	10 500	—	—	—	—	23 850	—	27 050	30 200	—	—	33 600	0·94
CR3-600	3400	10 500	—	—	—	—	23 850	—	27 050	30 200	—	—	33 700	0·99
CR3-800	3400	10 500	16 000	—	22 100	—	23 850	—	27 050	30 200	34 900	—	34 000	0·96
CR3-900	3400	10 600	14 800	17 000	20 100	22 450	—	26 000	27 050	30 200	32 000	36 300	34 000	1·62
CR3-950	3400	10 600	14 900	17 000	20 100	22 500	—	26 000	27 050	30 200	32 100	36 300	34 200	0·82
CR3-1100	3400	10 800	14 950	17 050	20 350	22 700	—	26 000	27 050	30 200	32 400	36 500	33 900	0·75
CR3-1650	3400	11 000	15 600	18 200	22 500	24 900	—	—	—	—	35 100	39 500	34 200	0·75
CR3-1750	3400	11 000	15 600	18 200	22 500	25 100	—	—	—	—	35 100	39 700	34 200	0·56

R, IR band of absorbed H_2O; F, impurity ferrous; U, M–O charge transfer; 5, Cr^{5+} bands; 6, Fe^{3+} bands (impurities); 7 and 8, Cr^{6+} bands; 1, 3 and 9, low field Cr^{3+} bands; 2, 4 and 10, high-field Cr^{3+} bands. σ, standard deviation of fitting in %; all bands in cm^{-1}. For the sample key see Table 1.

Results

X-ray diffractometry (XRD)

The mullite precursors are amorphous up to 600°C (Fig. 1). Above this temperature, weak reflections appear in the XRD patterns which are due to some small amount of crystalline Cr_2O_3. The Cr_2O_3 phase is present up to 1000°C. At 900°C, γ-Al_2O_3 forms, and becomes the only crystalline phase at 1100°C. The formation of mullite starts at 1250°C, as γ-Al_2O_3 disappears. XRD spectra taken from samples heat-treated above 1250°C show only the reflections of mullite. At 1750°C, besides mullite, a very low amount of α-Al_2O_3 can be detected.

Electron paramagnetic resonance spectroscopy (EPR)

Precursors calcined in the temperature range between 450 and 800°C show a strong and sharp EPR signal at $g_{eff} \approx 1{\cdot}96$ and a weak feature extending from $g \approx 5$ to $g \approx 2$ (Fig. 2), the former becoming anisotropic at Q-band frequencies. The strong signal near $g_{eff} = 1{\cdot}96$ disappears at calcination temperatures >800°C. Between 900 and 1000°C a glass-like Cr^{3+} EPR spectrum appears. Development of the typical Cr^{3+} EPR spectrum of mullite with characteristic features near $g_{eff} = 5$ is visible at higher temperatures (≥1250°C).

In the temperature range between 800 and 1100°C, an isotropic and broad EPR signal centred at $g_{eff} \approx 2$ can be additionally detected (Fig. 2). The intensity of this signal increases, if the EPR spectra are recorded at temperatures ≥310 K, due to the occurrence of crystalline Cr_2O_3.[7]

No additional EPR signal was detected down to 50 K, indicating the absence of additional Cr-bearing phases in the mullite precursors.

Optical absorption spectroscopy

As shown in Fig. 3, the optical absorption spectra of the precursors calcined between 450 and 1650°C were fitted by Gaussian curves. The differentiated peaks were labelled with numbers from 1

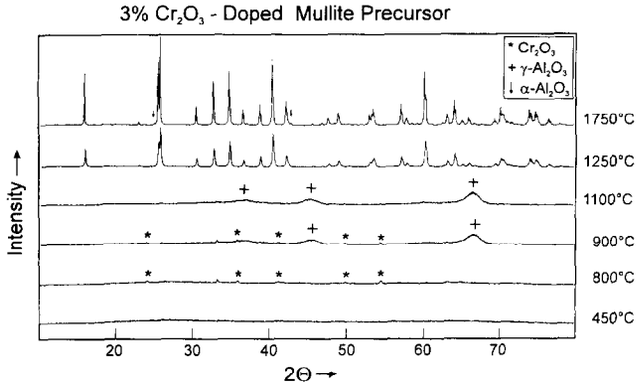

Fig. 1. Evolution of X-ray diffraction patterns of Cr-doped (3 wt%) mullite precursor with heat treatment temperature.

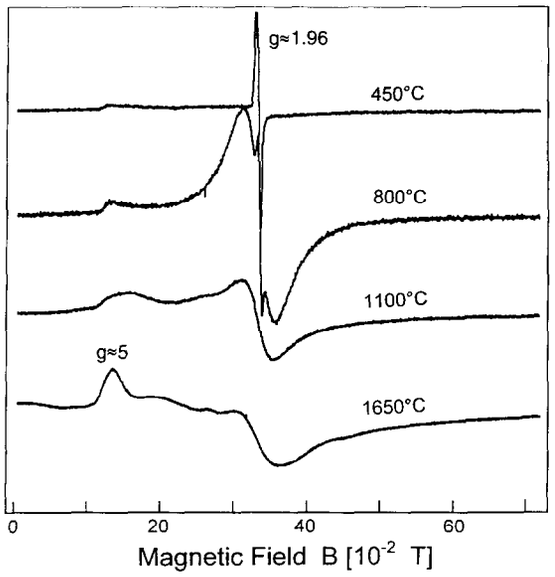

Fig. 2. Powder EPR spectra of Cr-doped (3 wt%) mullite precursors, heat-treated at 450, 800, 1100 and 1650°C. The spectra were taken at room temperature and 9.520 GHz.

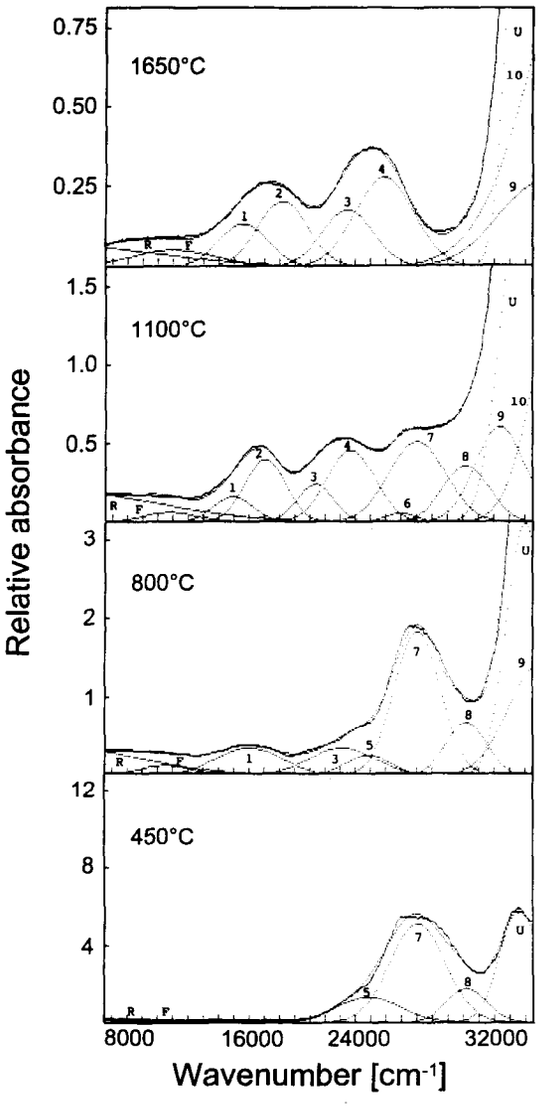

Fig. 3. Peak-fitted optical absorption spectra of Cr-doped (3 wt%) precursors, heat-treated at 450, 800, 1100 and 1650°C. For attribution of peak numbers see the text and Table 2.

to 10 (see the pattern of the 1100°C sample). They are listed in Table 2. Peaks 5, 7 and 8 are characteristic for the low temperature (450°C) sample, and are assumed to be the result of charge transfer transitions of Cr^{6+}. The corresponding EPR spectrum at this temperature, however, shows the presence of Cr^{5+} in the precursor. The electron configuration of Cr^{6+} and Cr^{5+} ions are $3d^0$ and $3d^1$, respectively. Cr^{5+} has an electron spin of $S = 1/2$ and is paramagnetic. It can therefore easily be detected by EPR. However, Cr^{6+} is diamagnetic and, hence, is not detectable by EPR. We believe that peak 5 belongs to Cr^{5+}, and peaks 7 and 8 to Cr^{6+}, which is in agreement with the yellow colour of the 450°C sample. The colour of precursors calcined at temperatures ≥800°C turns to green due to the appearance of Cr^{3+}. Above this temperature the intensities of optical absorption peaks 7 and 8, assigned to Cr^{6+}, decrease as the intensity of peak 5, assigned to Cr^{5+}, totally disappears.

Octahedrally coordinated Cr^{3+} generally displays two optical absorption peaks in the visible region due to the splitting of the F term. Sometimes an additional Cr^{3+} peak occurs in the UV region which results from the P term. This actually has been observed in the samples heat-treated at ≥800°C. The precursors calcined at 1650 and 1750°C have grey colour and their absorption spectra are equal to those of octahedrally coordinated Cr^{3+}, occurring in high and low field sites.[8] High and low field occupations of Cr^{3+} have also been observed in samples heat-treated between 900 and 1100°C, suggesting the evolution of a mullite-type short-range order in the precursors. However, Racah parameters (see below) show that this actually is not the case. Furthermore, peak 6 (Table 2) resolved in the spectra of these samples is believed to be due to impurity Fe^{3+} ions.[9]

Discussion

The EPR signal at $g_{eff} \approx 1.96$, appearing at calcination temperatures ≤1100°C, is connected with Cr doping, because it is not observed in undoped mullite precursors. The spin of the paramagnetic centre is assumed to be $S = 1/2$ and the g value indicates an electron centre. This signal is, therefore, assigned to Cr^{5+}. A paramagnetic centre with $S > 1/2$, e.g. Cr^{3+} with $S = 3/2$, can be excluded, because the Cr^{3+} EPR should not display a single line spectrum around $g_{eff} \approx 2$. The Cr^{5+} signal at $g_{eff} \approx 1.96$ can be simulated at both 9.5 and 35 GHz using an axial g tensor with $g_{x,y} = 1.960$ and $g_z = 1.946$, an effective spin $S = 1/2$ and a constant line width of 25×10^{-4} T. The frequency-independent line width indicates that Cr^{5+} occurs in a non-random environment. According to the EPR data only one type of coordination exists for Cr^{5+}.

Optical absorption spectra suggest that Cr^{5+} is present in larger amounts in the samples calcined at temperatures < 900°C, while Cr^{6+} persists up to ≤ 1100°C. Taking into account the ionic radii of Cr^{6+} (0.38 Å) and Cr^{5+} (0.43 Å),[10] both cations should be fourfold coordinated in these precursors. Substitution of Al^{3+} or Si^{4+} cations by Cr^{5+} or Cr^{6+} produces a charge surplus in the oxygen network which may be balanced by octahedral cation vacancies.

Although the Cr^{3+} EPR signal around $g_{eff} = 5$ is already present in the sample heat-treated at 450°C, its intensity is significant only at calcination temperatures > 800°C. This is in accordance with optical absorption data. Furthermore, from the absorption spectra a certain variation of slightly different distorted octahedral Cr^{3+} sites in the precursors can be deduced as high and low field sites.

The crystal field parameters 10 Dq and B for Cr^{3+} and Cr^{5+} cations in the Cr-doped precursors (Table 3) are in general agreement with literature data.[8] Racah parameters B of all samples are small, indicating a partly covalent bonding character of Cr^{3+} in the precursor matrix. The Racah parameter B of Cr^{3+} should be larger for high field and smaller for low field sites, respectively. This actually becomes true for samples heat-treated at 1650°C and at 1750°C, which comprise Cr-doped mullites. However, it does not hold for samples heat-treated in the temperature range between 900 and 1100°C where the formal application of the fitting procedure yielded high and low field sites with nearly the same Racah parameter (≈518 cm^{-1}). Therefore, we assume that strongly distorted Cr^{3+} sites which do not allow a

Table 3. Crystal field parameters 10 Dq and B of Cr-doped mullite precursors heat-treated at different temperatures

	Sample key							
	CR3-450	*CR3-600*	*CR3-800*	*CR3-900*	*CR3-950*	*CR3-1100*	*CR3-1650*	*CR3-1750*
Oct. Cr^{3+} 10 Dq	—	—	16000	14800/17000	14900/17000	14950/17050	15600/18200	15600/18200
B	—	—	601	513/515	500/521	524/537	717/654	717/679
Tet. Cr^{5+} 10 Dq	23850	23850	23850	—	—	—	—	—

Slash indicating both of high-field and low-field in cm^{-1}. Oct. = octahedral, Tet. = tetrahedral.

differentiation between high and low field Cr^{3+} positions can explain the above observations.

It is interesting to discuss the temperature-dependent mechanisms of Cr incorporation into the mullite precursors. The literature data on the hydrolysis behaviour of trivalent Cr^{3+} indicates that the kinetics of hydrolysis with Cr^{3+} are slow.[11] Slower kinetics facilitate occurrence of the gel network which results in the formation of polyanions by oxidation of Cr^{3+} to Cr^{6+}:[11]

$$[(OH)O_2Cr^{6+}\text{–}O\text{–}Cr^{6+}O_2(OH)]^0$$

On heating, deprotonation of the dimer occurs, yielding a gradual development of:

$$[Cr_2^{6+}O_5\,(OH)_2]^0 \rightarrow [Cr_2^{6+}O_6\,(OH)]^- + H^+$$

and

$$[Cr_2^{6+}O_6\,(OH)\,]^- \rightarrow [Cr_2^{6+}O_7]^{2-} + H^+$$

Reduction of $[Cr_2^{6+}O_7]^{2-}$ species at temperatures $\geq 800°C$ may result in the formation of crystalline $Cr_2^{3+}O_3$, as is observed by XRD of the calcined Cr-doped precursors.

Cr-doping of mullite precursors has a significant influence on the crystallization behaviour of the material. Undoped precursors prepared in exactly the same way as the Cr-doped precursors are amorphous up to $\approx 900°C$. At this temperature they crystallize to mullite and some small amount of γ-Al_2O_3. The nearly exclusive formation of mullite indicates that a small degree of phase separation into Al_2O_3- and SiO_2-rich areas occurred before mullite crystallization. Addition of chromium acetate in alcoholic solution, however, promotes this phase separation to such an extent that intermediate phases of γ-Al_2O_3 and Cr_2O_3-rich non-crystalline SiO_2 form prior to mullitization, similar to the case of type III mullite precursors.[4]

References

1. Hoffman, D., Roy, R. & Komarneni, S., Diphasic xerogels, a new class of materials: phases in the Al_2O_3–SiO_2 system. *J. Am. Ceram. Soc.*, **67** (1984) 468–71.
2. Komarneni, S., Suwa, Y. & Roy, R., Application of compositionally diphasic xerogels for enhanced densification: the system Al_2O_3–SiO_2. *J. Am. Ceram. Soc.*, **69** (1986) C-155–C-156.
3. Schneider, H., Okada, K. & Pask, J. A., *Mullite and Mullite Ceramics*. John Wiley & Sons, Chichester, 1994.
4. Schneider, H., Saruhan, B., Voll, D., Merwin, L. & Sebald, A., Mullite precursor phases. *J. Eur. Ceram. Soc.*, **11** (1993) 87–95.
5. Schneider, H., Voll, D., Schmücker, M., Saruhan, B., Schaller, T. & Sebald, A., Constitution of the γ-alumina phase in chemically produced mullite precursors. *J. Eur. Ceram. Soc.*, **13** (1994) 441–8.
6. Tanaka, K. L. & Kamiya, K., Electron spin resonance and optical absorption spectra of chromium in silica gels and glasses prepared by the sol–gel method. *J. Mater. Sci. Lett.*, **10** (1991) 1095–7.
7. Rager, H., Schneider, H. & Graetsch, H., Chromium incorporation in mullite. *Am. Mineral.*, **75** (1990) 392–7.
8. Ikeda, K., Schneider, H., Akasaka, M. & Rager, H., Crystal-field spectroscopic study of Cr-doped mullite. *Am. Mineral.*, **77** (1992) 251–7.
9. Marfunin, A. S., *Spectroscopy, Luminescence and Radiation Centers in Minerals*. Springer, Berlin, 1979.
10. Whittaker, E. J. W. & Muntus, R., Ionic radii for use in geochemistry. *Geochim. Cosmochim. Acta*, **34** (1970) 945–56.
11. Brinker, C. J. & Scherer, G. W., *Sol–Gel Science*. Academic Press, San Diego, CA, 1990.